AD-A112 260 MISSION RESEARCH CORP SANTA BARBARA CA F/G 17/9
ANGLE OF ARRIVAL FLUCTUATIONS IN A NUCLEAR DUST CLOUD PEDESTAL.(U)
AUG 81 C J LAUER DNA001-81-C-0162
UNCLASSIFIED MRC-N-476 DNA-TR-81-32 NL

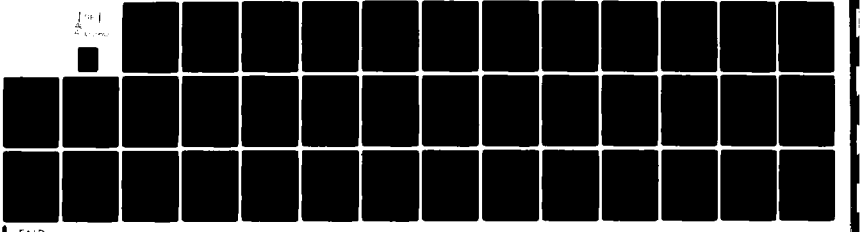

END
DATE FILMED
2-82
DTIC

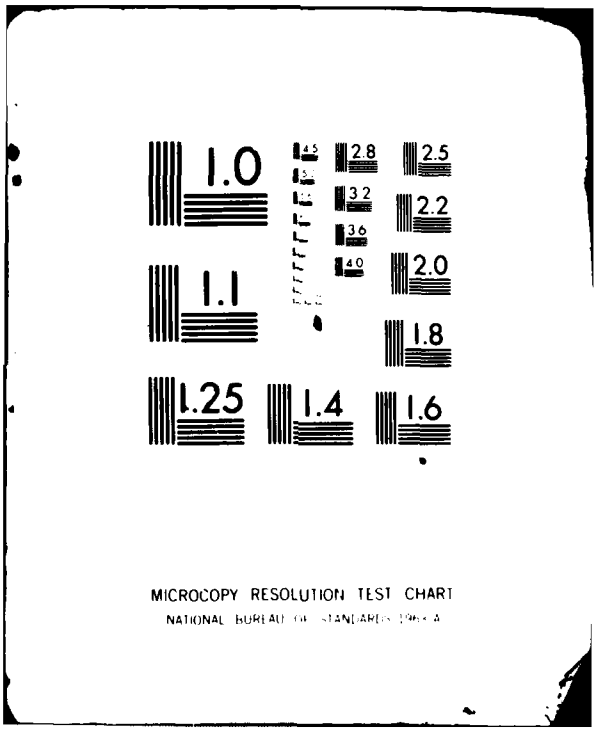
1.0
1.1
1.25
1.4
1.6
1.8
2.0
2.2
2.5
2.8
3.2
3.6
4.0
MICROCOPY RESOLUTION TEST CHART
NATIONAL BUREAU OF STANDARDS 1963-A

(12)

DNA-TR-81-32

ANGLE OF ARRIVAL FLUCTUATIONS IN A NUCLEAR DUST CLOUD PEDESTAL

Carl J. Lauer

Mission Research Corporation
P.O. Drawer 719
Santa Barbara, California 93102

1 August 1981

Technical Report

CONTRACT No. DNA 001-81-C-0162

THIS WORK SPONSORED BY THE DEFENSE NUCLEAR AGENCY
UNDER RDT&E RMSS CODE B310081466 S99QAXHC00027 H2590D.

Prepared for
Director
DEFENSE NUCLEAR AGENCY
Washington, D. C. 20305

Destroy this report when it is no longer needed. Do not return to sender.

PLEASE NOTIFY THE DEFENSE NUCLEAR AGENCY, ATTN: STTI, WASHINGTON, D.C. 20305, IF YOUR ADDRESS IS INCORRECT, IF YOU WISH TO BE DELETED FROM THE DISTRIBUTION LIST, OR IF THE ADDRESSEE IS NO LONGER EMPLOYED BY YOUR ORGANIZATION.

UNCLASSIFIED

SECURITY CLASSIFICATION OF THIS PAGE (When Data Entered)

REPORT DOCUMENTATION PAGE	READ INSTRUCTIONS BEFORE COMPLETING FORM
1. REPORT NUMBER: DNA-TR-81-32	2. GOVT ACCESSION NO.: AD-A112 200
3. RECIPIENT'S CATALOG NUMBER:	
4. TITLE (and Subtitle): ANGLE OF ARRIVAL FLUCTUATIONS IN A NUCLEAR DUST CLOUD PEDESTAL	5. TYPE OF REPORT & PERIOD COVERED: Technical Report
	6. PERFORMING ORG. REPORT NUMBER: MRC-N-476
7. AUTHOR(s): Carl J. Lauer	8. CONTRACT OR GRANT NUMBER(s): DNA 001-81-C-0162
9. PERFORMING ORGANIZATION NAME AND ADDRESS: Mission Research Corporation, P.O. Drawer 719, Santa Barbara, California 93102	10. PROGRAM ELEMENT, PROJECT, TASK AREA & WORK UNIT NUMBERS: Subtask S99QAXHC000-27
11. CONTROLLING OFFICE NAME AND ADDRESS: Director, Defense Nuclear Agency, Washington, D.C. 20305	12. REPORT DATE: 1 August 1981
	13. NUMBER OF PAGES: 38
14. MONITORING AGENCY NAME & ADDRESS(if different from Controlling Office)	15. SECURITY CLASS. (of this report): UNCLASSIFIED
	15a. DECLASSIFICATION/DOWNGRADING SCHEDULE: N/A

16. DISTRIBUTION STATEMENT (of this Report)

Approved for public release; distribution unlimited.

17. DISTRIBUTION STATEMENT (of the abstract entered in Block 20, if different from Report)

18. SUPPLEMENTARY NOTES

This work sponsored by the Defense Nuclear Agency under RDT&E RMSS Code B310081466 S99QAXHC00027 H2590D.

19. KEY WORDS (Continue on reverse side if necessary and identify by block number)

Fluctuations
Pedestal ANgle of Arrival
Turbulence
Radar
Dust Clouds
Nuclear Explosions

20. ABSTRACT (Continue on reverse side if necessary and identify by block number)

Angle-of arrival fluctuations from propagation through a nuclear dust cloud pedestal have been identified as a potential source of system degradation for a ground-based tracking radar.

This note investigates these angle-of-arrival fluctuations as measured by a 3 meter diameter lens type antenna operating at an RF wavelength of 3 centimeters. Since large uncertainties exist in the current knowledge of the dust

DD FORM 1 JAN 73 1473 EDITION OF 1 NOV 65 IS OBSOLETE

UNCLASSIFIED

SECURITY CLASSIFICATION OF THIS PAGE (When Data Entered)

20. ABSTRACT (Continued)

environment, this investigation is performed parametrically over what are estimated to be reasonable ranges of the key variables involved. The effects of antenna aperture taper, target elevation, radar height, dust material properties, dust distribution with height and also the size distribution of the irregularities are investigated.

TABLE OF CONTENTS

LIST OF ILLUSTRATIONS

FORMALISM/THEORY

BACKGROUND

Following Tatarskii[1], we consider the angular jitter measured by a lens type antenna where the scattered fields are given by the Rytov approximation. The use here of the Rytov approximation, which is a form of weak scatter theory, is justified in Appendix A. There it is shown that for the propagation paths considered, the estimated amplitude fluctuations are small compared to the level at which weak fluctuation theory breaks down. The development of a general equation capable of predicting results for the variation of all parameters of interest will be described. A Fortran code was written and validated to obtain results from this general formula.

The modeling geometry is shown in Figure 1. The radar antenna is immersed in a turbulent layer of dust and is tracking a target in angle. The angle estimator is assumed to correspond to the angular position of the target image intensity pattern in the image plane of the antenna. Due to the fluctuations induced by the turbulent propagation medium, the position of the target image will fluctuate. Tatarskii[1] has considered this problem for the case of an aperture with uniform illumination. We have modified his derivation to include the effect of an aperture amplitude taper.

From Appendix B, the mean squared deviation in the angle-of-arrival (in one plane only) is

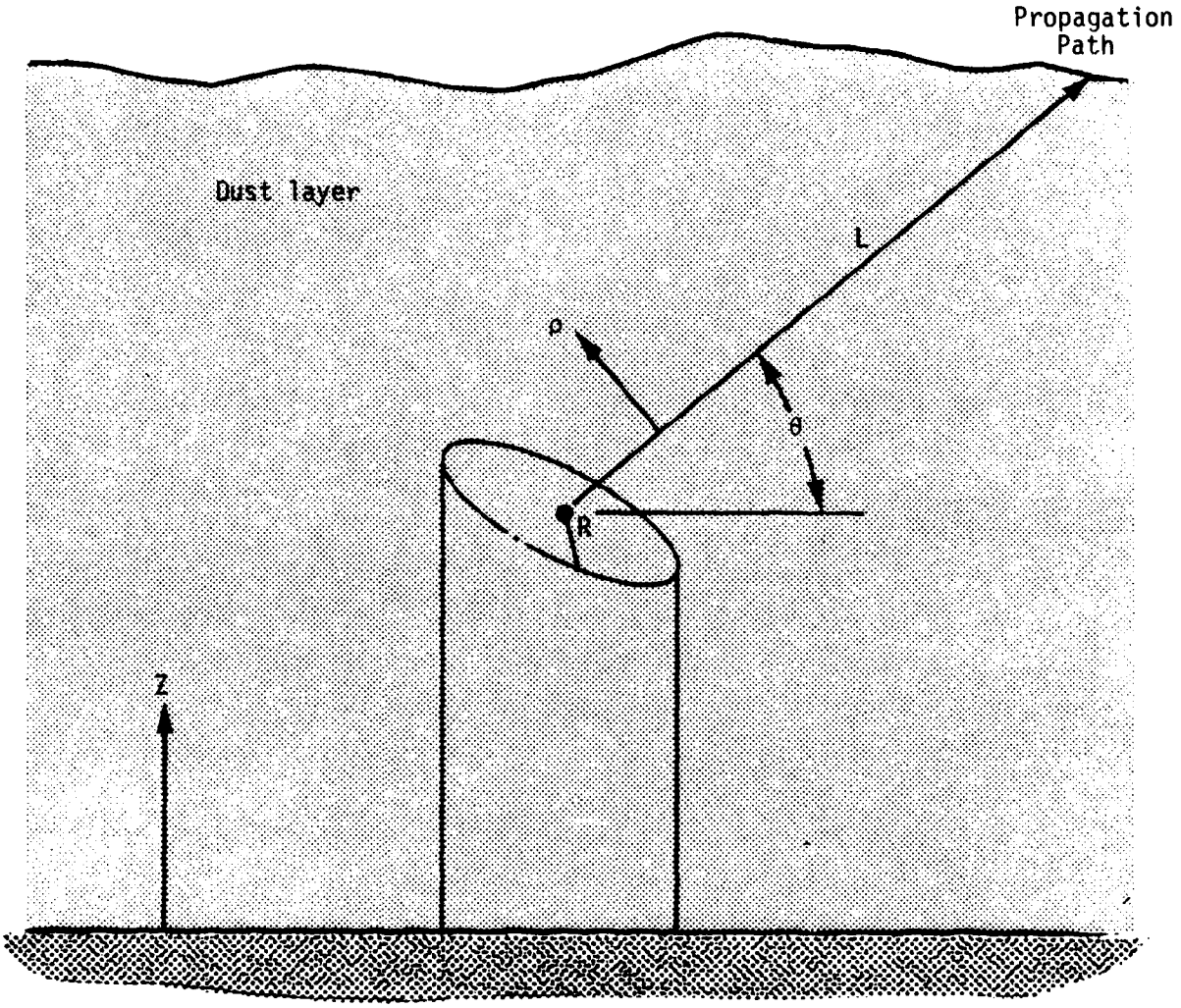

R = Radius of antenna aperture

θ = Target elevation

ρ = Distance measured transverse to the propagation path

Z = Altitude

L = Path length through the dust layer

Figure 1. Modeling geometry.

$$\sigma_\alpha^2 = \frac{\pi}{2k^2 A_e^2} \int_0^{2R} d\rho\ \rho\ I(\rho) \left[\frac{d^2 D(\rho)}{d\rho^2} + \frac{1}{\rho}\frac{dD(\rho)}{d\rho}\right] \quad (1)$$

where k = free space RF wave number.

A_e and $I(\rho)$ depend on the aperture design taper or weighting and are calculated from equations (B4), and (B10) respectively. $D(\rho)$ is the phase structure function evaluated at the antenna aperture as a function of distance (ρ) transverse to the propagation path.

POWER SPECTRAL DENSITY FUNCTION

We assume a power spectral density (PSD) which is locally homogeneous and isotropic and an index of refraction variance which is a function of altitude.

$$\Phi_n(K,Z) = \frac{L_o^3\ \Gamma(N/2)}{\pi^{3/2}\ \Gamma(N/2-3/2)} \frac{\Delta n^2(Z)}{(1+L_o^2 K^2)^{N/2}} \quad (2)$$

$$= \Phi_n^o(K)\ \Delta n^2(Z) \quad (3)$$

where

$\Phi_n(K,Z)$ = PSD of index of refraction fluctuations

$\Delta n^2(Z)$ = index of refraction variance of the air-dust medium as a function of altitude

L_o = outer scale of turbulence

K = spatial wave number

N = 3-D power law exponent.

Using equation (3) and equations (1.50) and (8.11) from Reference 2, $D(\rho)$ may be expressed as

$$D(\rho) = 4\pi^2 k^2 \int_0^\infty dK\, K\, [1-J_0(K\rho)]\, \Phi_n^0(K) \qquad (4)$$

$$\cdot \int_0^L dX'\, \Delta n^2(X') \left\{1+\cos\left[\frac{K^2(L-X')}{k}\right]\right\}$$

where $J_0(K\rho)$ = Bessel function of the first kind of zero order, and the integration in X' is over the propagation path from the layer boundary to the antenna at slant range L away. (See Figure 1)

Making a change of variables from X' to X such that X = L-X' and using

$$\frac{d^2J_0(K\rho)}{d\rho^2} + \frac{1}{\rho}\,\frac{dJ_0(K\rho)}{d\rho} = -K^2J_0(K\rho),$$

we may differentiate $D(\rho)$ to obtain

$$\frac{d^2D(\rho)}{d\rho^2} + \frac{1}{\rho}\,\frac{dD(\rho)}{d\rho} = 4\pi^2k^2 \int_0^\infty dK\, K^3\, J_0(K\rho)\, \Phi_n^0(K) \qquad (5)$$

$$\cdot \int_0^L dX\, \Delta n^2(X)\, \left[1 + \cos\left(\frac{K^2X}{k}\right)\right] \quad .$$

Here the integration in X is from the antenna to the layer boundary. Substituting (5) into (1) we obtain

$$\sigma_\alpha{}^2 = \frac{2\pi^3}{A_e{}^2} \int_0^{2R} d\rho\, \rho\, I(\rho) \int_0^\infty dK\, K^3\, \Phi_n^0(K)\, J_0(K\rho)\, H(K) \qquad (6)$$

where

$$H(K) = \int_0^L dX\ \Delta n^2(X)\ \left[1 + \cos\left(\frac{K^2 X}{k}\right)\right] \quad . \tag{7}$$

LOADING PROFILES

Let the target elevation angle be θ with $\zeta = \csc(\theta)$, and the antenna height Z_R. For uniform loading over the layer

$$H(K) = \Delta n_{ou}^2 \int_0^L dX\ \left[1 + \cos\left(\frac{K^2 X}{k}\right)\right] = \Delta n_{ou}^2\ L\left[1 + \frac{k}{K^2 L} \sin\left(\frac{K^2 L}{k}\right)\right] \tag{8}$$

where $L = \zeta(Z_L - Z_R)$, and Z_L is the height of the dust layer.

For exponential loading

$$H(K) \approx \Delta n_{oe}^2\ \zeta \int_{Z_R}^{\infty} dZ\ e^{-2Z/h_s}\ \left[1 + \cos\left(\frac{K^2 \zeta Z}{k}\right)\right]$$

$$= \frac{\Delta n_{oe}^2}{2}\ \zeta h_s\ e^{-2Z_R/h_s} \left[1 + \frac{\cos\left(\frac{K^2 \zeta Z_R}{k}\right) - \left(\frac{K^2 \zeta h_s}{2k}\right) \sin\left(\frac{K^2 \zeta Z_R}{k}\right)}{1 + \left(\frac{K^2 \zeta h_s}{2k}\right)^2}\right] \tag{9}$$

where the mean and also the root-mean-square deviation in the index of refraction are assumed to vary as $\exp(-Z/h_s)$ so that Δn_e^2 varies as $\exp(-2Z/h_s)$. Δn_{ou}^2 and Δn_{oe}^2 in equations (8) and (9) are, respectively, the index of refraction variances in the dust laden air medium for the uniform and exponential layers at zero altitude.

VARIANCE OF THE INDEX OF REFRACTION OF THE MEDIUM

Following Reference 3, we assume that the mean value for the index of refraction of the medium is given by the Clausius-Mossotti formula

$$n = 1+n_1 \approx 1 + \frac{3}{2}\left(\frac{n_b^2-1}{n_b^2+2}\right)\frac{\rho_m}{\rho_b} \tag{10}$$

and that the root-mean-square deviation in n is equal to 1/2 of n_1

$$\Delta n = 1/2\ n_1 \quad . \tag{11}$$

Here n_b is the index of refraction of the bulk material which can be closely approximated by using its real part only. ρ_m, ρ_b are the densities of the medium and bulk material, respectively. The assumption $\Delta n = 1/2\ n_1$ corresponds to the worst case situation, which is expected at early times after the pedestal cloud has formed. As the turbulent energy in the cloud is transferred into heat, the factor of 1/2 will eventually become much smaller.

Substituting (10) into (11) we obtain

$$\Delta n = 3/4\left(\frac{n_b^2-1}{n_b^2+2}\right)\frac{\rho_m}{\rho_b} \tag{12}$$

This may be restated in a convenient form by making use of the fact that ρ_m is generated by a scoured layer of thickness ΔZ of the bulk material whose density is ρ_b. Then for uniform loading

$$\Delta n_{ou} = \frac{3}{4}\left(\frac{n_b^2-1}{n_b^2+2}\right)\frac{\Delta Z}{Z_L} \tag{13}$$

and for exponential loading

$$\Delta n_{oe} = \frac{3}{4}\left(\frac{n_b^2-1}{n_b^2+2}\right)\frac{\Delta Z}{h_s} \quad . \tag{14}$$

The variance of the index of refraction of the medium is then obtained by taking the square of (13) or (14) as desired.

WORKING EQUATION

The parametric investigation was performed through the evaluation of equation (6) which we restate by substituting for ϕ_n^o from equation (2)

$$\sigma_\alpha^2 = \frac{2\pi^{3/2} L_o^3 \Gamma(N/2)}{A_e^2 \Gamma(N/2 - 3/2)} \times \int_0^{2R} d\rho\ \rho\ I(\rho) \int_0^{\infty} dK\ K^3\ J_o(K\rho)\ H(K)\ (1+L_o^2K^2)^{-N/2} \tag{15}$$

where A_e and $I(\rho)$ are given by equations (B12) through (B17) and H(K) is taken from (8) or (9) as desired. The two integrations in equation (15) were computed numerically.

RESULTS

A list of parameters affecting the angle-of-arrival problem which have been studied is given below. Note there are two parameters (antenna aperture illumination, radar height) which the designer could possibly control. (Changing the environment by relocating the radar site or by modifying the terrain from which the dust is lofted are other obvious considerations.)

- CHARACTERIZATION OF THE ENVIRONMENT
  - PSD
    - Turbulence Outer Scale Size (L_o)
    - 3-D Power Law Exponent (N)
    - Bulk Index of Refraction (n_b)
  - Dust Loading Profile
    - Uniform
    - Exponential
    - Scoured Layer Removed (ΔZ)
- RADAR OPERATION
  - Antenna Aperture Effects (Illumination Functions)
  - Target Elevation (θ), Radar Height (Z_R)

NOMINAL CASE

Unless otherwise specified, we assume the following nominal conditions:

Exponential loading, h_s = 6 m
2 cm of caliche scoured (n_b = 2.2)
Kolmogorov spectrum, N = 11/3
L_o = 10 m, θ = 90°
Uniform aperture illumination
Radar height, Z_R = 0 m

For these conditions we find $\sigma_\alpha \approx 1.7$ mrad.

VARIATIONS ABOUT THE NOMINAL

Figure 2 demonstrates the variation in σ_α with outer scale and the 3-D power law exponent of the PSD for an exponentially loaded layer. Variations in σ_α attributable to uncertainty in L_o can approach factors of $\pm$ 2 for $1<L_o<100$ m for a given N. For a fixed choice of outer scale, a variation in N from 3 to 5 can produce variations of $\pm \sqrt{3}$ in σ_α.

Figure 3 is a repeat of Figure 2 except that the 2 cm of scoured caliche has been distributed uniformly over a 100 m layer. It is observed that the values of σ_α predicted for the uniform layer are about a factor of 3 smaller than for the exponential layer with a 6 m scale height. This can be explained as follows. Let the mean turbule diameter for a given L_o and N be equal to d. Then in traversing a layer thickness Z, σ_α^2 will be proportional to the variance in the index of refraction for an average turbule (Δn^2) times the number of turbules passed (m). Thus

$$\frac{\sigma_{\alpha,u}^2}{\sigma_{\alpha,e}^2} \approx \frac{\Delta n_u^2}{\Delta n_e^2} \frac{m_u}{m_e} \tag{16}$$

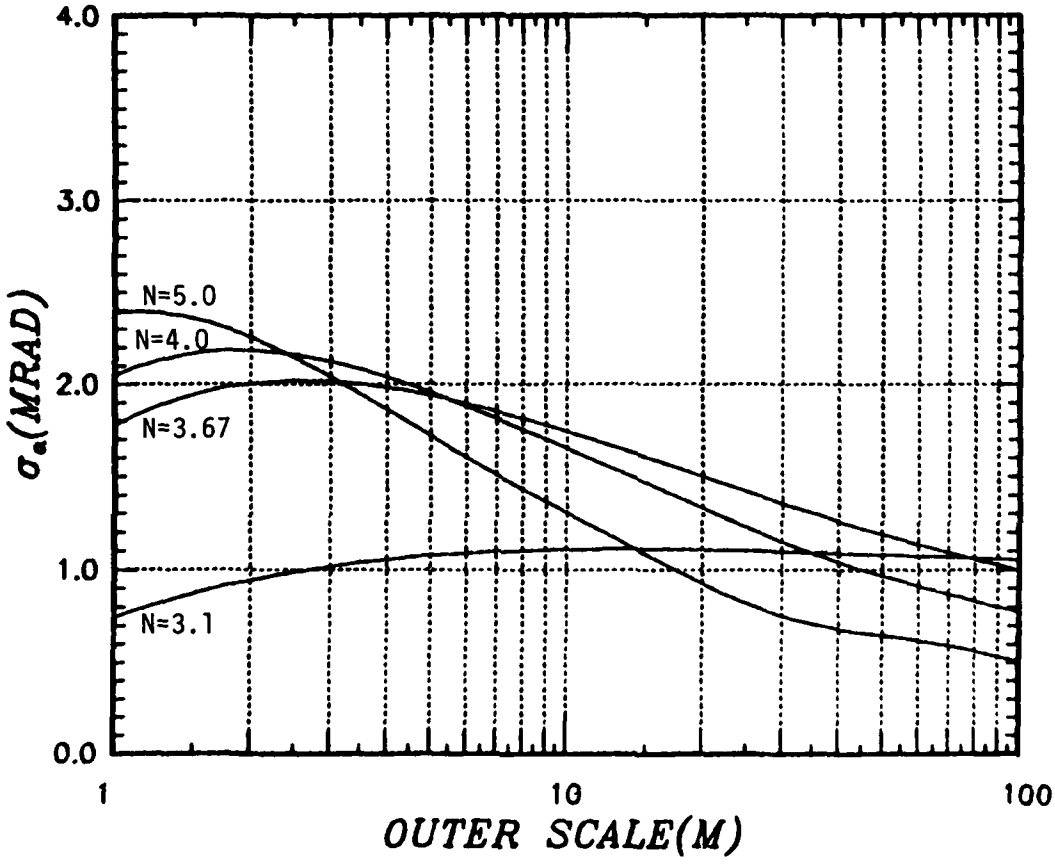

Figure 2. σ_α vs outer scale and 3-D power law exponent (N) for an exponential dust layer.

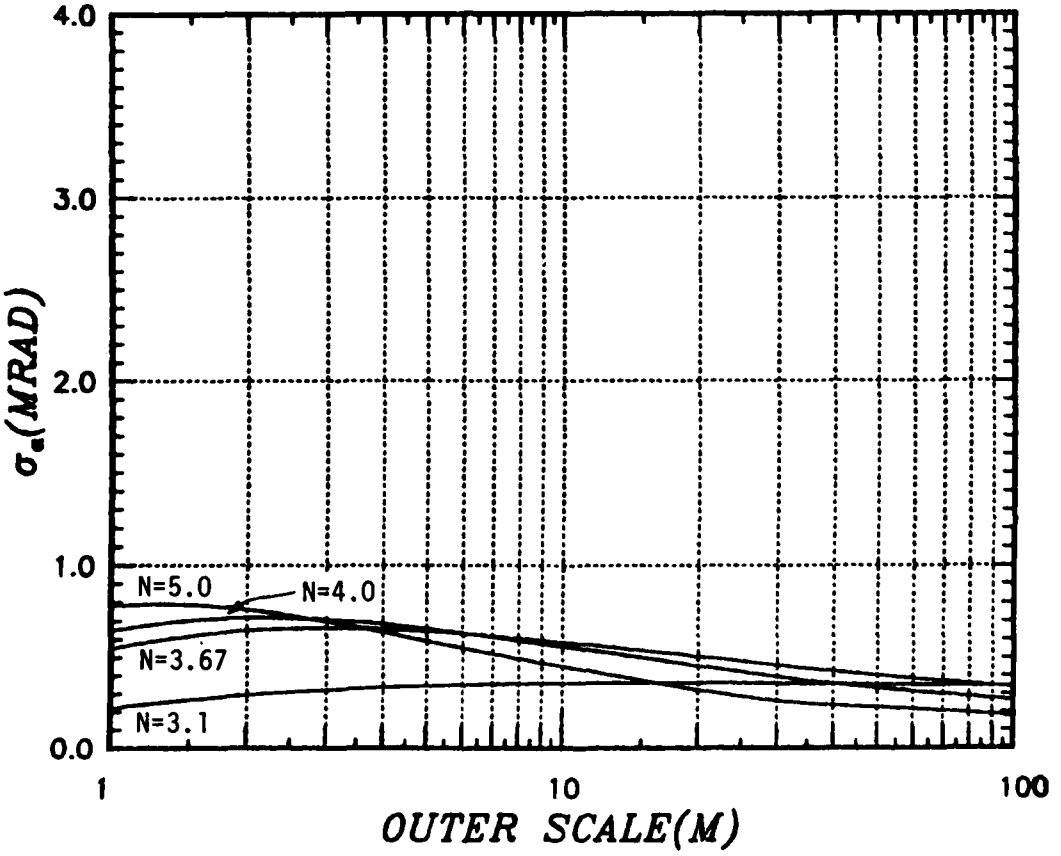

Figure 3. σ_α vs outer scale and 3-D power law exponent (N) for a uniformly loaded layer 100m thick.

where the subscripts u and e refer to uniform and exponential respectively. For a constant layer $m_u \approx Z_L/d$ and for an exponential layer $m_e \approx h_s/d$. Also, referring to equations (13) and (14)

$$\frac{\Delta n_u^2}{\Delta n_e^2} \approx \frac{h_s^2}{Z_L^2} \quad . \tag{17}$$

Then

$$\frac{\sigma_{\alpha,u}}{\sigma_{\alpha,e}} \approx \sqrt{\frac{h_s^2 Z_h}{Z_L^2 h_s}} = \sqrt{\frac{h_s}{Z_L}} \approx \frac{1}{4} \quad , \tag{18}$$

approximating the numerical result of 1/3 quoted earlier. The results for the uniform layer have been compared with a previous result published by Thompson in Reference 4. They are found to be in excellent agreement when the differences in the scoured layers assumed are taken into account.

In Figure 4 we have investigated variations of σ_α with scale height for exponential loading. The increase in σ_α with decreasing scale height may be explained by the same reasoning as was used above to compare the results for the uniform and exponential layers. The variation of h_s about the nominal 6 m value results in fluctuations of a factor of $\approx$ 0.5 to 1.7 in σ_α.

Figure 5 shows the effects of target elevation and also radar height on σ_α. For a decrease in target elevation from the nominal case of 90° down to 15° we see a factor of about 2 increase in σ_α. This rise results from an increase in path length through the dust with decreasing look angle. For a fixed target elevation and our nominal 6 m dust scale height, we note a decrease in σ_α by a factor of $\approx$ .7 when the antenna face is lifted 2 m above the ground. This decrease in σ_α is caused simply by the fact that a large quantity of the former propagation environment is

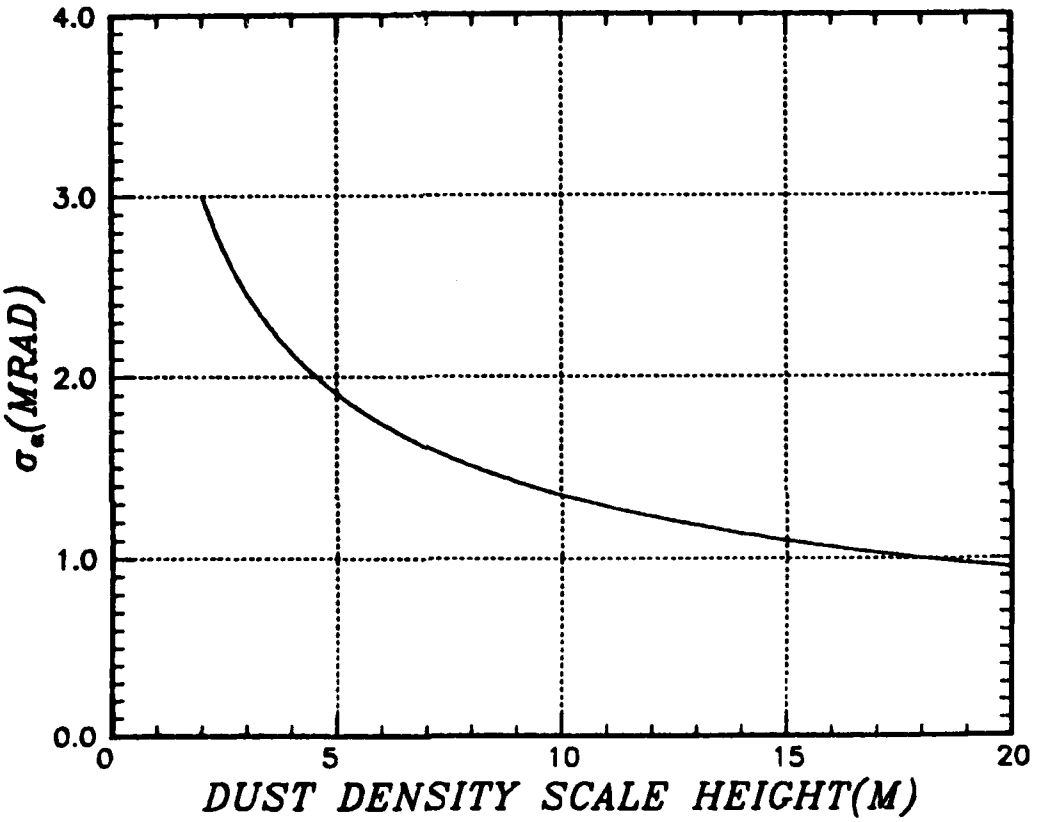

Figure 4. σ_α vs dust density scale height.

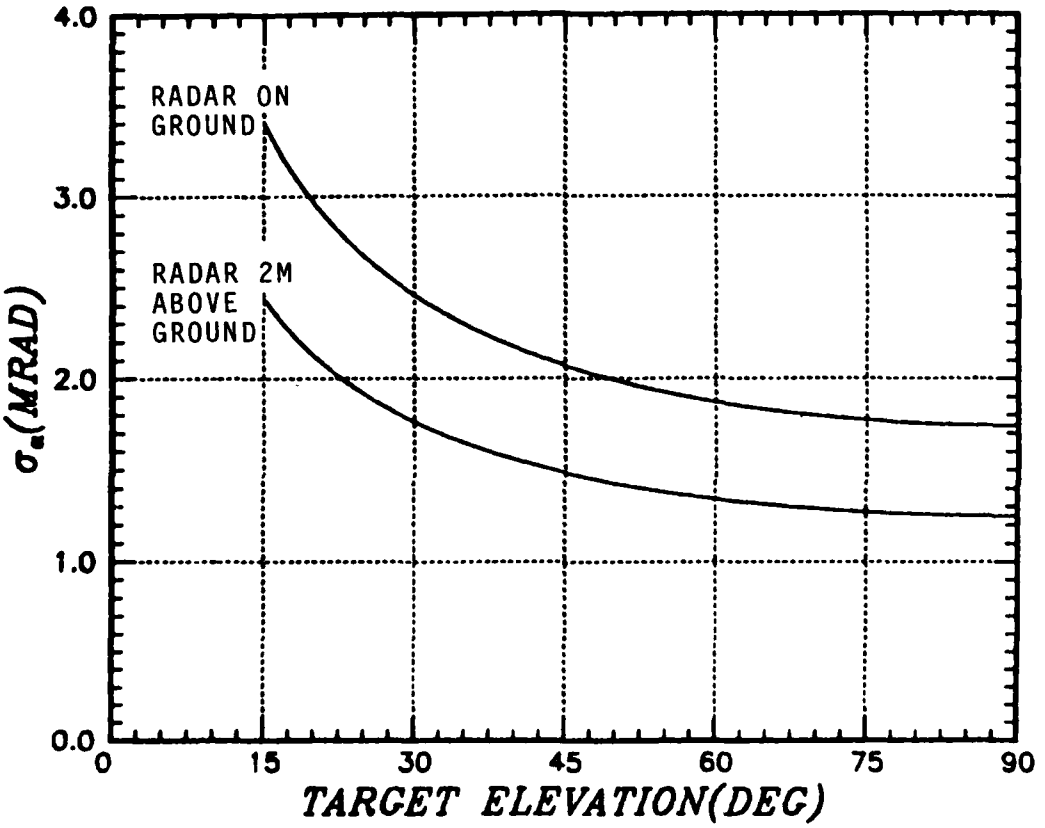

Figure 5. σ_α vs target elevation and radar height.

now below the antenna and has no effect. It should be realized that for smaller scale heights this factor would become more significant, and for large scale heights the effect of a 2 m radar height would be negligible.

The three separate aperture amplitude design tapers are plotted in Figure 6, with their corresponding peak sidelobe levels also listed for reference. The resultant variations in σ_α as a function of design taper and outer scale are shown in Figure 7. It is seen that with increasing amplitude taper, corresponding to greater sidelobe suppression, there results an increase in σ_α. Thus there exists a tradeoff between sidelobe suppression and angle of arrival jitter. The peak increase in σ_α is a factor of $\approx$ 1.6. This increase occurs because a tapered aperture gives lower sidelobes at the expense of a somewhat broader beam and a broader beam in space lets in rays from a wider range of angles. The possible significance of this effect remains to be investigated.

The effect of varying material properties when the scoured layer thickness is held constant is obtained directly from equation (13) or (14)

$$\sigma_\alpha \approx \Delta n \approx \frac{n_b^2-1}{n_b^2+2} \quad . \tag{19}$$

Table 1 lists the bulk indices of refraction and resulting variations in $(n_b^2-1)/(n_b^2+2)$ for representative materials of interest. We note a resultant factor of $\approx$ .6 to 1.4 in σ_α about the nominal case.

Table 1. Material Variations. (From Gutsche's data, Reference 5.)

Material	n_b	$\frac{n_b^2-1}{n_b^2+2}$
Dry, sandy soil	1.58	.33
* Caliche	2.20	.56
Wet Clay	3.34	.77

* Nominal Case

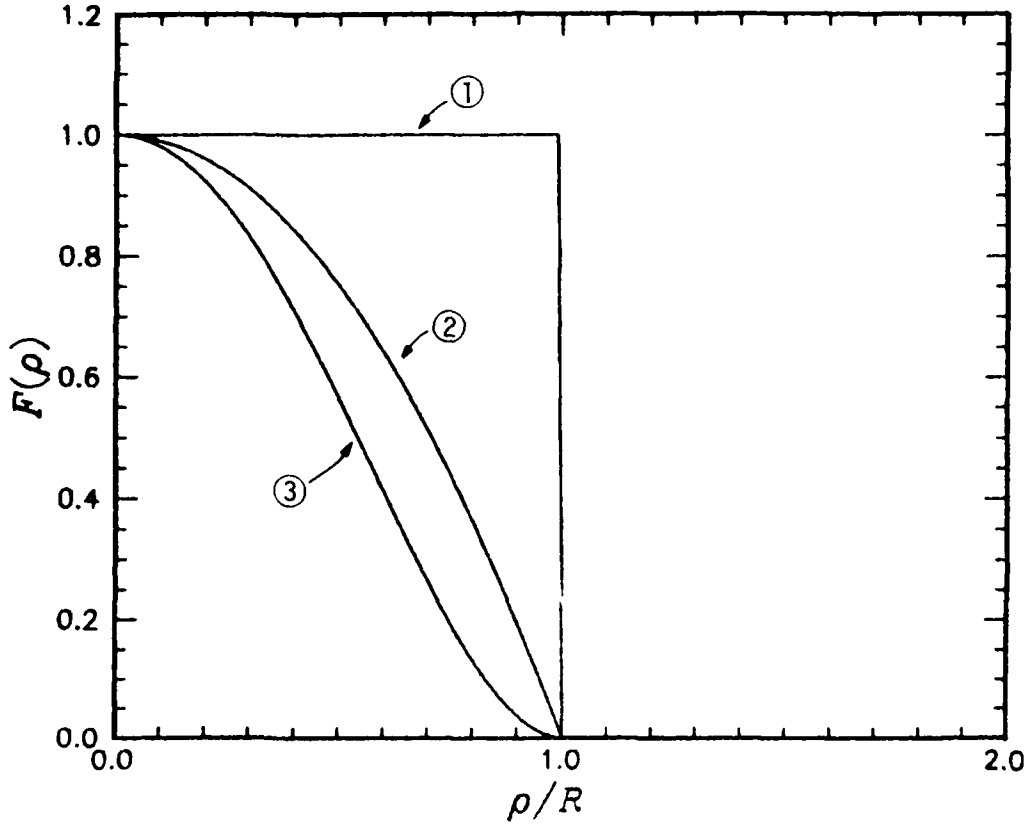

		Sidelobe Level (dB)
①	$F(\rho) = \text{Const}$	18
②	$F(\rho) = (1-\rho^2/R^2)$	25
③	$F(\rho) = (1-\rho^2/R^2)^2$	31

Figure 6. Aperture amplitude design tapers.

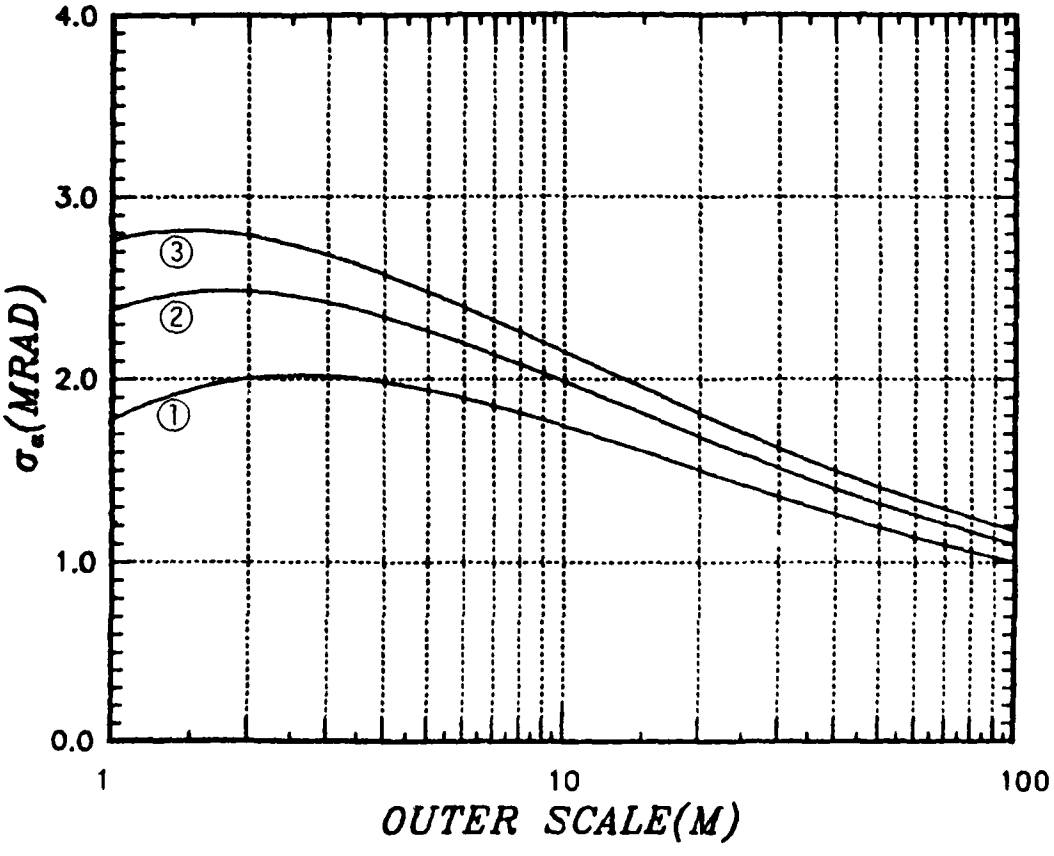

① $F(\rho) = \text{Const}$

② $F(\rho) = (1-\rho^2/R^2)$

③ $F(\rho) = (1-\rho^2/R^2)^2$

Figure 7. σ_α **vs aperture taper design and outer scale.**

CONCLUSIONS

Results are summarized in Table 2. It is seen that for the nominal conditions of 2 cm of scoured surface we predict about 2 mrad of jitter. However, notice that σ_α is directly proportional to the amount of surface removed and this quantity is highly uncertain. Variations in other quantities lead to factors of ≈ ±2 about the nominal case. In addition, with specially selected (worst case) parameter variations, as much as 10 mrad of jitter is possible with the 2 cm of scoured surface.

It is appropriate to consider the amount of signal attenuation predicted for this dust loading. From Reference 5, Figure 1 we note that for 2 cm of surface removed, there is less than 15 dB of 2-way signal attenuation for the worst case combinations of material composition and its size distribution in the medium. Thus, a couple of milliradians of jitter may be possible under conditions for which attenuation is not severe.

Table 2. Results.

VARIATIONS RELATIVE TO NOMINAL CASE		
σ_α(nom) ≈ 1.7 mrad		
QUANTITY VARIED	$\frac{\sigma_\alpha \text{ (min)}}{\sigma_\alpha \text{ (nom)}}$	$\frac{\sigma_\alpha \text{ (max)}}{\sigma_\alpha \text{ (nom)}}$
PSD	.3	1.4
Loading (scoured layer removed)	Directly Proportional	
Material properties	.6	1.4
Scale Height	.5	1.7
Radar Height	.7	1.0
Target Elevation	1.0	2.0
TRADEOFF BETWEEN SIDELOBE SUPPRESSION AND JITTER		

REFERENCES

1. Tatarskii, V. I., The Effects of the Turbulent Atmosphere on Wave Propagation, TT-68-50464, National Science Foundation, Washington, D.C., 1971.

2. Tatarskii, V. I., Wave Propagation in a Turbulent Medium, McGraw Hill, New York, 1961.

3. "Communication Degradation Issues Relevant to a Massive Attack Environment," Mission Research Corporation, Unpublished.

4. Thompson, J. H., "Sensitivity of Dust Propagation Effects in a Nuclear Pedestal Region," Kaman Tempo, April 1981.

5. Gutsche S. L., "X-Band Attenuation From a Nuclear Dust Cloud Pedestal: Bounding Calculations and Determination of Sensitivity to Key Parameters," MRC-N-464, Mission Research Corporation, May 1981.

6. Ishimaru, A. K., Wave Propagation and Scattering in Random Media; Volume 2, Multiple Scattering, Turbulence, Rough Surfaces and Remote Sensing, Academic Press, 1978.

APPENDIX A
JUSTIFICATION FOR THE USE OF WEAK SCATTER THEORY

The formalism which has been developed utilizes results from weak scatter theory. According to Reference 6 weak fluctuation theory is valid when the log-amplitude variance is less than about .2 to .5. For the case of a Kolmogorov spectrum, the log-amplitude variance is given by

$$\sigma_\chi^2 = .586 \frac{\Delta n^2 k^{7/6} L^{11/6}}{L_o^{2/3}} \qquad \text{(A1)}$$

for uniform loading and a path length L. We approximate the nominal exponential layer (h_s = 6 m) by a uniform layer of height 6 m. Δn^2 is taken to correspond to that at ground level for the nominal conditions. This should yield a conservative estimate. Then

$$L = 6 \text{ m}$$
$$L_o = 10 \text{ m}$$
$$k = (2\pi/.03)\text{m}^{-1}$$
$$\Delta n = \frac{3}{4}\left(\frac{2.2^2-1}{2.2^2+2}\right)\frac{.02}{6}$$

and

$$\sigma_\chi^2 \approx 3.4\ 10^{-3} \quad .$$

This is two orders of magnitude smaller than the value for which weak fluctuation theory breaks down. It is safe to assume that σ_χ^2 will be smaller than .2 for all cases we have considered, so that the use of weak scatter theory is justified.

BLANK PAGE

APPENDIX B

ANGLE OF ARRIVAL FLUCTUATIONS FOR AN ANTENNA WITH A TAPERED APERTURE AMPLITUDE DESIGN

As stated earlier, we have assumed that the relevant angle estimator is that of the angular coordinates of the "center of gravity" of the intensity pattern of the target image in the focal plane of the antenna. Following Tatarskii[1], the angular deflection of the center of gravity of the image (in one plane only) is given by

$$\sigma_o = \frac{\frac{1}{k} \iint_{\Sigma} \mathrm{Im}\left[\psi(\eta',\xi') \frac{\partial \psi(\eta',\xi')}{\partial \eta'}\right] F^2(\eta',\xi') d\xi' d\eta'}{\iint_{\Sigma} \left|\psi(\eta',\xi')\right|^2 F^2(\eta',\xi')\, d\eta' d\xi'} \qquad \text{(B1)}$$

where

k = free space RF wave number

$\psi(\eta',\xi')$ = scattered field at the antenna aperture in the Rytov approximation

$F(\eta',\xi')$ = antenna aperture amplitude design taper

Σ = aperture area

(This may be obtained from Reference 1 page 287, equation (13) by letting $\psi \mapsto F\psi$.)

Letting $\psi = A_o \exp(X+iS)$, where

X = log-amplitude of the scattered field

S = phase of the scattered field

we may write equation (B1) as

$$\alpha_o = \frac{-1}{k} \frac{\iint_\Sigma F^2(\eta',\xi')\exp(2X)\,\frac{\partial S(\eta',\xi')}{\partial \eta'}\,d\eta'd\xi'}{\iint_\Sigma F^2(\eta',\xi')\exp(2X)\,d\eta'd\xi'} \tag{B2}$$

It is seen in equation (B2) that the main contribution to α_o is from phase fluctuations since $\alpha_o = 0$ for S = constant. Then to first order we may neglect the effect of amplitude fluctuations and

$$\alpha_o = \frac{-1}{kA_e} \iint_\Sigma F^2(\eta',\xi')\,\frac{\partial S(\eta',\xi')}{\partial \eta'}\,d\eta'd\xi' \tag{B3}$$

where

$$A_e = \text{"effective area"} = \iint_\Sigma F^2(\eta',\xi')d\eta'd\xi' \quad . \tag{B4}$$

The mean squared deviation in α is then

$$\sigma_\alpha{}^2 = \langle \alpha_o{}^2 \rangle$$

$$= \frac{1}{k^2 A_e{}^2} \iint_\Sigma \iint_\Sigma F^2(\eta',\xi')F^2(\eta'',\xi'') \left\langle \frac{\partial S(\eta',\xi')}{\partial \eta'} \frac{\partial S(\eta'',\xi'')}{\partial \eta''} \right\rangle$$

$$d\eta'd\xi'd\eta''d\xi'' \quad . \tag{B5}$$

The expectation of the phase derivatives may be written in terms of the phase structure function as

$$\left\langle \frac{\partial S(\eta',\xi')}{\partial \eta'} \frac{\partial S(\eta'',\xi'')}{\partial \eta''} \right\rangle = \frac{\partial^2}{\partial \eta' \partial \eta''} \langle S(\eta',\xi')\, S(\eta'',\xi'') \rangle$$

$$= \frac{\partial^2}{\partial\eta'\partial\eta''} B(\eta'-\eta'',\ \xi'-\xi'') = -\frac{\partial^2}{\partial\eta'^2} B(\eta'-\eta'',\xi'-\xi'')$$

$$= \frac{1}{2}\ \frac{\partial^2}{\partial\eta'^2} D(\eta'-\eta'',\xi'-\xi'') \qquad \text{(B6)}$$

where it is assumed that the phase correlation function B and the phase structure function D depend only on the distance between the points (η',ξ') and (η'',ξ''). Substituting (B6) into (B5), we may write

$$\sigma_\alpha^2 = \frac{1}{2k^2A_e^2} \iint_\Sigma \iint_\Sigma \frac{\partial^2 D(\eta'-\eta'',\xi'-\xi'')}{\partial\eta'^2} F^2(\eta',\xi')\ F^2(\eta'',\xi'')$$

$$d\eta' d\xi' d\eta'' d\xi'' \quad . \qquad \text{(B7)}$$

We now make a change of variable from (η'',ξ'') to (η,ξ) such that $\eta = \eta'-\eta''$, $\xi = \xi'-\xi''$. Keeping in mind that the area Σ is a circular aperture of radius R,

$$\sigma_\alpha^2 = \frac{1}{2k^2A_e^2} \iint_{\sqrt{\eta^2+\xi^2}<2R} d\eta d\xi\ \frac{\partial^2 D(\eta,\xi)}{\partial\eta^2}$$

$$\cdot \iint_\Sigma d\eta' d\xi'\ F^2(\eta',\xi')\ F^2(\eta'-\eta,\xi'-\xi) \quad . \qquad \text{(B8)}$$

Changing to polar coordinates (ρ,ϕ) and assuming that the structure function is locally isotropic so that

$$D(\eta,\xi) = D\left(\sqrt{\eta^2+\xi^2}\right) \quad \text{and}$$

$$\frac{\partial^2 D(\rho)}{\partial\eta^2} = \frac{\eta^2}{\rho^2}\ \frac{d^2D(\rho)}{d\rho^2} + \frac{\xi^2}{\rho^3}\ \frac{dD(\rho)}{d\rho}$$

$$= \cos^2\phi \frac{d^2D(\rho)}{d\rho^2} + \frac{1}{\rho}\sin^2\phi\ \frac{dD(\rho)}{d\rho}$$

we obtain

$$\sigma_\alpha^2 = \frac{1}{2k^2A_e^2} \int_0^{2R} d\rho\ \rho \int_0^{2\pi} d\phi\ \left[\cos^2\phi \frac{d^2D(\rho)}{d\rho^2} + \frac{1}{\rho} \sin^2\phi \frac{dD(\rho)}{d\rho}\right] I(\rho) \qquad (B9)$$

where

$I(\rho)$ = "illumination function"

$$= 4 \int_0^{\cos^{-1}(\rho/2R)} d\phi' \int_{\rho/2\cos\theta}^{R} d\rho'\rho'\ F^2(\rho')\ F^2\left[\sqrt{(\overline{\rho}'-\overline{\rho})^2}\right] \quad . \qquad (B10)$$

Performing the integration over ϕ in equation (B9) we have

$$\sigma_\alpha^2 = \frac{\pi}{2k^2A_e^2} \int_0^{2R} d\rho\ \rho\ I(\rho) \left[\frac{d^2D(\rho)}{d\rho^2} + \frac{1}{\rho} \frac{dD(\rho)}{d\rho}\right] \quad . \qquad (B11)$$

The geometry for the integration of equation (B10) is shown in Figure B1. We evaluate equations (B4) and (B10) for 3 separate amplitude tapers*

Case 1:

$F(\rho) = 1$

$$A_e = \pi R^2 \qquad (B12)$$

$$I(\rho) = 2R^2 \left[\cos^{-1}(\rho/2R) - (\rho/2R)\sqrt{1-\rho^2/4R^2}\right] \qquad (B13)$$

---

* $I(\rho)$ was evaluated analytically for Case 1, and numerically for Cases 2 and 3. For Cases 2 and 3 $I(\rho)$ was then expressed in terms of polynomial expansions through use of a curve fitting routine.

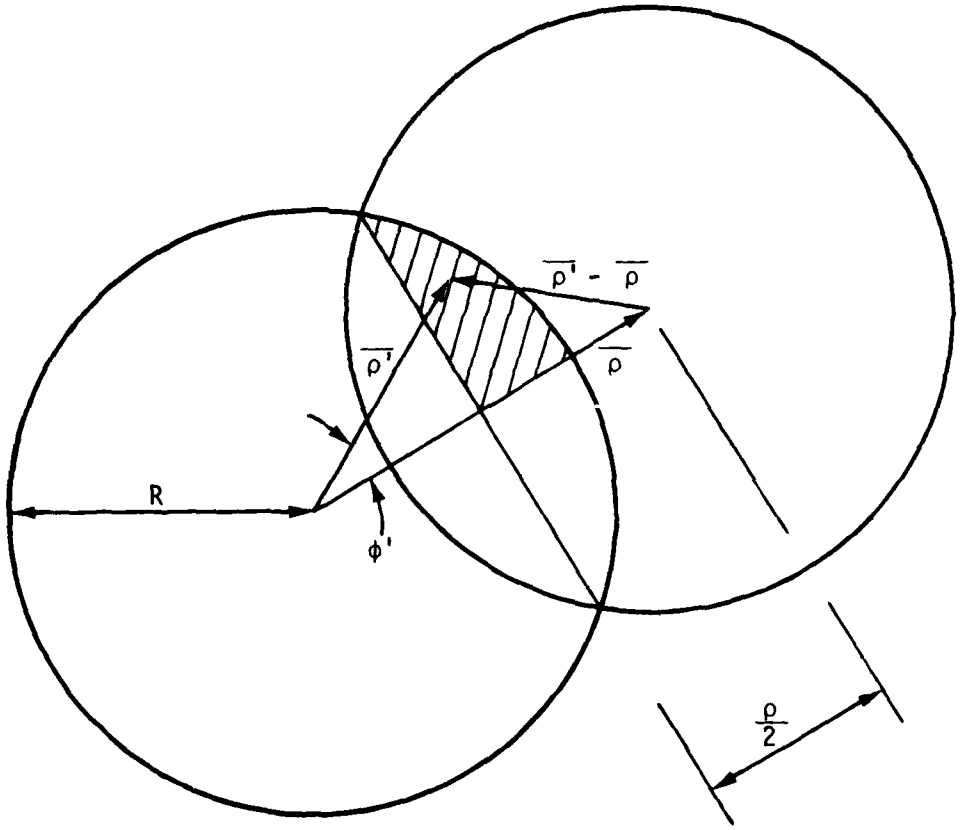

Figure B1. Geometry for the integration of equation (B10).

Case 2:

$$R(\rho) = 1-\rho^2/R^2$$

$$A_e = \pi R^2/3 \tag{B14}$$

$$I(\rho) = R^2 \left[A_2+B_2(\rho/R) + C_2(\rho^2/R^2) + D_2(\rho^3/R^3) + E_2(\rho^4/R^4) + F_2(\rho^5/R^5)\right] \tag{B15}$$

Case 3:

$$F(\rho) = (1-\rho^2/R^2)^2$$

$$A_e = \pi R^2/5 \tag{B16}$$

$$I(\rho) = R^2 \left[A_3+B_3(\rho/R + C_3(\rho^2/R^2) + D_3(\rho^3/R^3) + E_3(\rho^4/R^4) + F_3(\rho^5/R^5)\right] \tag{B17}$$

where

$A_2 = .6220536$
$B_2 = .1518489$
$C_2 = -1.859473$
$D_2 = 1.699667$
$E_2 = -.5666203$
$F_2 = .06177243$

$A_3 = .3445954$
$B_3 = .1363949$
$C_3 = -1.785527$
$D_3 = 2.168312$
$E_3 = -1.01252$
$F_3 = .1681695$

The unitless form $I(\rho)R^2/A_e^2$ is plotted for Cases 1, 2 and 3 in Figure B2.

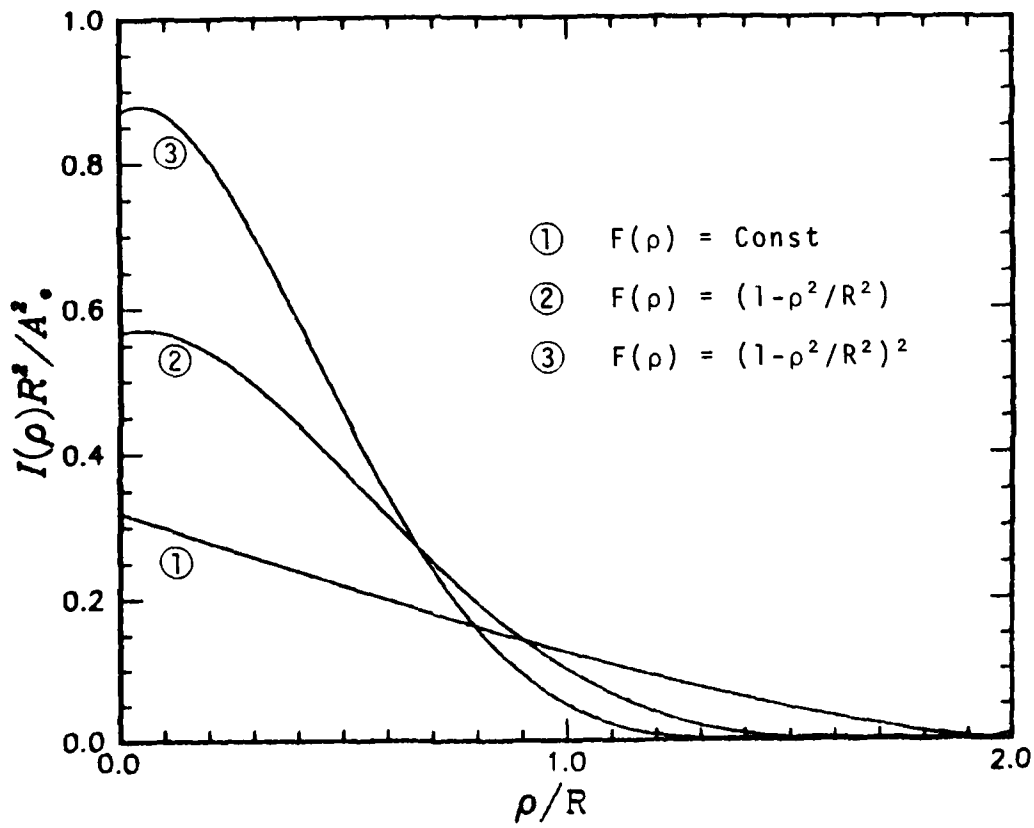

Figure B2. $I(\rho)R^2/A_e^2$ vs ρ/R for three aperture design tapers.

BLANK PAGE

DISTRIBUTION LIST

DEPARTMENT OF DEFENSE

Assistant Secretary of Defense
Comm, Cmd, Cont & Intell
ATTN: Dir of Intelligence Sys, J. Babcock

Defense Nuclear Agency
ATTN: NAFD
ATTN: STNA
ATTN: RAEE
ATTN: NATD
4 cy ATTN: TITL
6 cy ATTN: RAAE

Defense Technical Information Ctr
12 cy ATTN: DD

Field Command
Defense Nuclear Agency
ATTN: FCPR, J. McDaniel

Field Command
Defense Nuclear Agency
Livermore Br
ATTN: FCPRL

Interservice Nuclear Wpns Sch
ATTN: TTV

Joint Chiefs of Staff
ATTN: C3S, Evaluation Ofc
ATTN: C3S

Joint Strat Tgt Planning Staff
ATTN: JLTW-2
ATTN: JLA

DEPARTMENT OF THE ARMY

Atmospheric Sciences Lab
U.S. Army Electronics R&D Cmd
ATTN: DELAS-EO, F. Niles

BMD Advanced Technology Ctr
Department of the Army
ATTN: ATC-O, W. Davies
ATTN: ATC-T, M. Capps

BMD Systems Cmd
Department of the Army
2 cy ATTN: BMDSC-HW

Harry Diamond Labs
Department of the Army
ATTN: DELHD-NW-R, R. Williams
ATTN: DELHD-NW-P

U.S. Army Chemical Sch
ATTN: ATZN-CM-CS

U.S. Army Comm R&D Cmd
ATTN: DRDCO-COM-RY, W. Kesselman

U.S. Army Materiel Dev & Readiness Cmd
ATTN: DRCLDC, J. Bender

DEPARTMENT OF THE ARMY (Continued)

U.S. Army Missile Intelligence Agcy
ATTN: YSE, J. Gamble

U.S. Army Nuclear & Chemical Agcy
ATTN: Lib

U.S. Army TRADOC Sys Analysis Actvy
ATTN: ATAA-TDC
ATTN: ATAA-PL
ATTN: ATAA-TCC, F. Payan, Jr.

DEPARTMENT OF THE NAVY

Joint Cruise Missiles Proj Ofc
Department of the Navy
ATTN: JCMG-707

Naval Electronic Systems Cmd
ATTN: PME 117-2013, G. Burnhart
ATTN: PME 106-4, S. Kearney
ATTN: PME 117-211, B. Kruger
ATTN: Code 3101, T. Hughes
ATTN: PME 117-20
ATTN: PME 106-13, T. Griffin
ATTN: Code 501A

DEPARTMENT OF THE AIR FORCE

Aerospace Defense Cmd
Department of the Air Force
ATTN: DC, T. Long

Air Force Geophysics Lab
ATTN: OPR, H. Gardiner
ATTN: OPR-1
ATTN: LKB, K. Champion
ATTN: OPR, A. Stair
ATTN: S. Basu
ATTN: PHP
ATTN: PHI, J. Buchau
ATTN: R. Thompson

Air Force Weapons Lab
Air Force Systems Command
ATTN: SUL
ATTN: NTYC
ATTN: NTN

Air Force Wright Aeronautical Lab
ATTN: W. Hunt
ATTN: A. Johnson

Air Logistics Cmd
Department of the Air Force
ATTN: OO-ALC/MM

Air Weather Service, MAC
Department of the Air Force
ATTN: DNXP, R. Babcock

Ballistic Missile Ofc
Air Force Systems Command
ATTN: ENSN, J. Allen

DEPARTMENT OF THE AIR FORCE (Continued)

Assistant Chief of Staff
Studies & Analyses
Department of the Air Force
ATTN: AF/SASC, W. Keaus
ATTN: AF/SASC, C. Rightmeyer

Deputy Chief of Staff
Ops Plans and Readiness
Department of the Air Force
ATTN: AFXOKCD
ATTN: AFXOKS
ATTN: AFXOXFD
ATTN: AFXOKT

Rome Air Dev Ctr
Air Force Systems Command
ATTN: EEP

Strategic Air Cmd
Department of the Air Force
ATTN: DCXT
ATTN: NRT
ATTN: DCXR, T. Jorgensen
ATTN: XPFS
ATTN: DCX

OTHER GOVERNMENT AGENCY

Institute for Telecom Sciences
Natl Telecom & Info Admin
ATTN: W. Utlaut
ATTN: A. Jean
ATTN: L. Berry

DEPARTMENT OF DEFENSE CONTRACTORS

Aerospace Corp
ATTN: T. Salmi
ATTN: J. Straus
ATTN: R. Slaughter
ATTN: V. Josephson
ATTN: I. Garfunkel
ATTN: D. Olsen
ATTN: N. Stockwell
ATTN: S. Bower

BDM Corp
ATTN: L. Jacobs
ATTN: T. Neighbors

Berkeley Rsch Associates, Inc
ATTN: J. Workman

ESL, Inc
ATTN: J. Marshall

General Rsch Corp
ATTN: J. Ise, Jr.
ATTN: J. Garbarino

Institute for Defense Analyses
ATTN: J. Aein
ATTN: H. Gates
ATTN: H. Wolfhard
ATTN: E. Bauer

DEPARTMENT OF DEFENSE CONTRACTORS (Continued)

Kaman Tempo
ATTN: T. Stephens
ATTN: DASIAC
ATTN: W. McNamara
ATTN: W. Knapp

McDonnell Douglas Corp
ATTN: J. Moule
ATTN: G. Mroz
ATTN: W. Olson
ATTN: N. Harris
ATTN: R. Halprin

Meteor Comm Consultants
ATTN: R. Leader

Mission Research Corp
ATTN: S. Gutsche
ATTN: R. Bogusch
ATTN: D. Sappenfield
ATTN: F. Fajen
ATTN: Tech Lib
ATTN: R. Hendrick
ATTN: R. Kilb
4 cy ATTN: C. Lauer
5 cy ATTN: Doc Con

Mitre Corp
ATTN: A. Kymmel
ATTN: C. Callahan
ATTN: G. Harding
ATTN: B. Adams

Mitre Corp
ATTN: M. Horrocks
ATTN: J. Wheeler
ATTN: W. Hall
ATTN: W. Foster

Pacific-Sierra Rsch Corp
ATTN: E. Field, Jr.
ATTN: F. Thomas
ATTN: H. Brode

Physical Dynamics, Inc
ATTN: E. Fremouw

Physical Rsch, Inc
ATTN: R. Deliberis

R & D Associates
ATTN: R. Lelevier
ATTN: R. Turco
ATTN: H. Ory
ATTN: B. Gabbard
ATTN: M. Gantsweg
ATTN: W. Wright
ATTN: C. Greifinger
ATTN: W. Karzas
ATTN: F. Gilmore
ATTN: P. Haas

Science Applications, Inc
ATTN: L. Linson
ATTN: D. Hamlin
ATTN: E. Straker
ATTN: C. Smith

DEPARTMENT OF DEFENSE CONTRACTORS (Continued)

Science Applications, Inc
ATTN: SZ

Science Applications, Inc
ATTN: J. Cockayne

Sylvania Systems Gp
ATTN: R. Steinhoff
ATTN: I. Kohlberg
ATTN: J. Concordia

Technology International Corp
ATTN: W. Boquist

Computer Sciences Corp
ATTN: F. Eisenbarth

DEPARTMENT OF DEFENSE CONTRACTORS (Continued)

SRI International
ATTN: W. Chesnut
ATTN: R. Leadabrand
ATTN: D. Neilson
ATTN: J. Petrickes
ATTN: R. Livingston
ATTN: G. Price
ATTN: W. Jaye
ATTN: C. Rino
ATTN: A. Burns
ATTN: R. Tsunoda
ATTN: G. Smith
ATTN: M. Baron

BLANK PAGE